



OPEN Infiltration capacity and salinization dynamics of the ishaqi aquifer with sustainable groundwater desalination strategies in central Iraq

Najah M. L. Al Maimuri¹, Zaidoon Najah Mahdi Al Mamouri², Layth Abdulameer³✉, Awad Jadooe³, Hayder. J. Kurji⁴ & Ahmed N. Al-Dujaili⁵✉

Given the shortage of surface water supplies caused by the construction of dams in the upstream countries of the Tigris River, which has reduced Iraq's share of water, the increasing demand for water, and climate change, groundwater has emerged as a critical and essential water resource. This study aims to find the infiltration capacity and salinization of groundwater in the unconfined aquifer relationship and sustainable remediation of aquifer storage in the north Baghdad Ishaqi area of central Iraq in 2024. GIS and Surfer software were used. Ten soil and groundwater samples were extracted from sites randomly distributed throughout the area of 410 km², with 10 double-ring infiltrometer tests being conducted at the same sites. The results of the on-site tests revealed that the central part of the area was characterized by coarse-grained soil, higher infiltration capacity, and higher groundwater concentrations, which ranged between 70–82%, 87–183 mm/hr., and 2,050–4,200 m/L, respectively. The opposite was the case in the northern and southern parts of the area. The desalination process of the Ishaqi aquifer requires a double injection of water with pumping rates of 1, 2, 3, 4, and 5 m³/s of water to reduce salinity from 4,500 to 500 mg/L of 108 m³ aquifer volume for periods of 8,800, 4,620, 3,140, 2,360, and 1,780 days, respectively. These periods were greatly reduced when the outflow rate became twice the inflow rate. The mitigation equation was derived from basic assumptions of enclosed aquifer and homogenous mixing. A good coincidence between theoretical and measured concentrations was obtained. The study concluded that there is a direct mathematical relationship between aquifer salination and deep filtration with a correlation factor of 0.998, which led to high total dissolved solids (TDS) accumulations in the groundwater. The desalination process is possible and requires 2–10 years depending on pumping rates. The saline aquifer mitigation procedure is a successful and beneficial long-term tool.

Keywords Infiltration capacity, Groundwater desalination, Soil texture, Total dissolved salt, Pumping rates

The rise in groundwater salinity above the worldwide recommended concentrations, for various reasons, has become a global problem as 16% of the total land area of the Earth suffers from groundwater salinization, which leads to environmental, economic, and social problems [1]. To discuss the reasons for the increase in groundwater salinity, 520 scientific studies were collected by [2]. The most important papers were focused on seawater intrusion and the infiltration of irrigation water.[2]. In recent years, the Ishaqi region has been the home of the *Al-Ishaqi Irrigation Project*, which uses water for different activities, i.e., agricultural, urban and industrial. Since farmers have recently begun consuming more water than their water supply allows, they have

¹Building and Construction Technologies Engineering Department, College of Engineering and Engineering, Technologies, Al-Mustaqbal University, Babylon, Hillah 51001, Iraq. ²Architecture Engineering Department, University of Babylon, Babylon, Iraq. ³Department of Civil Engineering, College of Engineering, University of Kerbala, Karbala 56001, Iraq. ⁴Department of Mechanical Engineering, College of Engineering, University of Kerbala, Karbala 56001, Iraq. ⁵Petroleum Engineering Department, Amirkabir University of Technology, No. 350, Hafez Ave, Valiasr Square, Tehran, Iran. ✉email: laith.saeed@uokerbala.edu.iq; ahmed.noori203@aut.ac.ir

turned to consuming groundwater [3]. Accordingly, they have suffered from groundwater salinization of the unconfined aquifer in its central section, such that the water has become unfit for drinking and agriculture use for unspecified reasons. Therefore, this study was undertaken to reveal the causes of salinization and develop appropriate solutions to desalinate the groundwater. The infiltration rates in sandy soils are usually higher in silt–clay texture soils because of light texture and high porosity. Also, the increase in the concentration of salts in groundwater accelerates the infiltration rate [4]. Several experiments were conducted over 20 years in the Huang-Huai-Hai alluvial plain, China, to measure the movement of salts through saline soils containing a subsurface clay layer. It was found that clay soil layers with a thickness of > 1 m reduced the deep filtration rate and, thus, helped to increase soil salinization [5]. Consequently, Improving infiltration capacity provides a feasible solution for remediating deficient groundwater aquifers. Groundwater is more difficult to monitor and manage than surface water, but it is critical to ecosystems and human needs. Managed infiltration restores aquifers, promoting sustainable recharge and balancing demand. This method must consider hydrological, ecological, and social variables. Effective implementation necessitates stakeholder participation and science-based integrated groundwater management (IGM). Infiltration-based managed aquifer recharge, which uses basins, trenches, or ponds, is commonly used to increase recharge and reduce salinity. These strategies are commonly used in dry places around the world for sustainable groundwater management [6]. Over the last 60 years, increased groundwater extraction and advances in water treatment have fueled the global expansion of managed aquifer recharge (MAR). This research gives the first global estimate of MAR volume and examines its evolution across different types, technologies, and laws. MAR is becoming increasingly important for protecting groundwater from climatic stress and extremes. Scientific research has improved MAR design, efficiency, and water quality management, particularly in urban and mining environments. Despite annual growth of ~5%, MAR still amounts for ~1–2.4% of global extraction, with potential to surpass 10% with greater application [7]. Groundwater salinization may be controlled via abstraction, desalination, and recharge technologies. Brackish water is extracted, desalinated, and then recharged back into the aquifer. The findings indicate that enhanced recharge significantly reduces groundwater salinity, whereas increasing abstraction has no effect [8]. To desalinate aquifer water and control groundwater salinization, a recharge technique based on well placement is implemented. Freshwater is pumped directly into the toe of the saltwater wedge, where it is most effective at repelling incoming seawater. When recharge rates are the same, both point and line injection systems function identically. This technique increases desalination by pushing saline water seaward under hydraulic pressure. Saltwater repulsion efficiency improves when recharge is combined with flow barriers near the coast that extend deep into the aquifer [9]. MAR is the purposeful recharge of an aquifer for later recovery or environmental benefits and represents a valuable method for sustainable water resources management. The study encompasses a survey and an analysis of case studies which apply flow and transport models to evaluate MAR. The observed modeling objectives include the planning or optimization of MAR schemes as well as the identification and quantification of geochemical processes during injection, storage and recovery. The water recovery efficiency and the impact of the injected water on the ambient groundwater are further objectives investigated [10]. Rising populations and water demand have contributed to global groundwater depletion, particularly in arid and semi-arid countries that rely on aquifers. MAR has developed as an important approach for restoring groundwater, with California serving as a prime example. The state is experiencing significant overdraft difficulties, with over 100 km³ lost since 1962, forcing widespread MAR implementation. Common methods include injection wells, infiltration basins, and agricultural MAR, like as winter field flooding. California's numerous MAR uses highlight both traditional traditions and novel approaches to future groundwater management [11]. Geochemical, hydrochemical and stable isotope analyses were conducted in the Karamay area, China, to evaluate the groundwater quality and to identify the causes of excessive salinization. The addition of irrigation water without any groundwater withdrawal caused an increase in the groundwater level by 6.9 m between 1997 and 2009 and an increase in the concentrations of Na-Cl and Na-SO₄ salts, where the TDS values were between 0.5–65 gm/L, with higher values in the low-lying areas, characterized by surface water-bearing lenses because they provide greater amounts for deep filtration. Rainwater lenses are an important source of recharge for saline groundwater [12]. To know the dynamics of the work, monthly samples of soil and water were collected, and groundwater levels were monitored [13, 14]. It was found that the mixing point between lens water and groundwater was small and changed over a long time scale. This is known as the slow transient oscillatory flow regime [15]. Mixing processes are faster near the groundwater level, which is characterized by its response to recharge and evaporation in less than a day. The salinity of the soil may become more than the salinity of the groundwater due to the capillary action and the accumulation of salts in it after water evaporation, as well as the incomplete infiltration of fresh water [16]. Excess irrigation water is one of the most important reasons for groundwater salinization due to deep infiltration. A numerical mathematical model was developed that links deep infiltration of recycled saline water and the degree of concentration of TDS in a saturated zone. The results showed that the increase in salt concentrations in groundwater was about 12 mg/L/year. The study concluded that this value decreased when the irrigation system was converted from flood irrigation to drip irrigation by about 60% [17]. In the Datong Basin, North China, an analysis of trace elements and isotopes was conducted. The water was dominated by sodium bicarbonate, with high hydrochemical concentrations of TDS and low concentrations of the solids Na-SO₄, Na-Cl, and Na-HCO₃.

The main components of groundwater adjacent to the mountains were Mg-CO₃ and Ca-CO₃. The decomposition of alumina, exchange of cations, and dissolution of evaporites (halite, marabillite, and gypsum) are the main causes of groundwater salinization, with the effect of rapid recharge by irrigation water. The study recommended groundwater pumping for irrigation and salt flushing to maintain the quality of the groundwater [18]. The hydrochemical properties of 73 groundwater and 11 surface water samples in the Manas River Basin, NW China, were tested to determine the causes and sources of excessive groundwater salinity ranging from 0.2 to 11.91 gm/L. These high concentrations are found in agricultural areas irrigated with groundwater.

The evapotranspiration contribution was 5.87% and 32.7% for groundwater and surface water salinization, respectively. The study concluded that the causes of increased salinity were infiltration of the irrigated lands by groundwater and by evapotranspiration [19]. A laboratory experiment was conducted on three columns of saline soil (clay, silty and sandy) in cylinders with a diameter of 10 cm and a height of 30 cm. The salinity was fixed for all three. Different irrigation systems were applied, and the HYDRUS 1D model was used to analyze the results. These showed that intermittent irrigation was the best method for removing salts from the soil by deep infiltration in unsaturated clay soils by removing 75% of the salt concentrations. The same process did not make any difference in removing salts in sandy soils. Therefore, it is recommended that farmers use intermittent irrigation in the reclamation of clay soils and limit the excessive groundwater salinization, if time permits [20].

A layer of clay soil was used to desalinate the saline groundwater migrating from the unconfined aquifer to the confined aquifer in the lower layers. Chemical tests of the infiltrated groundwater, which lasted 212 days, proved that the clay layer reduced the salinity of the infiltrated water and did not contribute to the desalination process by completely removing the salt concentrations in it. This occurred due to the ion exchange of the element Na^+ with the elements Ca^{2+} and Mg^{2+} by approximately 30%. The removal of sodium occurred due to the ion exchange of the element Na^+ [21]. Researchers have been able to measure the hydraulic conductivity of unsaturated soil above an aquifer. The hydraulic conductivity is calculated based on the depth of water accumulated by deep infiltration into the groundwater storage over 24 h using Horton's law and the power model [22]. To reduce soil salinity, it is necessary to increase the deep infiltration of irrigation water. One of the most important techniques for this is to spread a layer of wind sand over the original soil surface. Laboratory results have shown the best option is adding a layer of sand amounting to 8% in weight ratio of the original soil, as it increases salt infiltration by 55% after seven days of operating the irrigation system [23]. The hydraulic conductivity in the saturated zone above the shallow groundwater was estimated based on the water infiltration system using Darcy's law and the physio-mechanical properties of soil. The practical part of this study was conducted in an area close to the currently considered study area in central Iraq [24].

Topography plays a major role in controlling the physical properties of soil and groundwater salinity because it controls the distribution and values of deep infiltration of water [25]. Moreover, the accumulation of surface water due to topography increases the infiltration rates and the concentration of surface water salinity [26]. All these variables are reflected in the growth of vegetation. Moreover, climate changes in temperature and rainfall directly affect the level of deep infiltration, which, in turn, changes the concentration of groundwater salinity [27]. In an experiment, three samples of melted glacial water with salt concentrations of 5, 10 and 15 mg/L were prepared and applied respectively to a saline soil column and the salinity of the soil infiltration water was measured. The results showed that higher salinity water caused higher infiltration of salt infiltration. In general, a 30 cm thick desalination layer was obtained and the use of salt infiltration of water with different salinity levels led to an acceleration of the infiltration process and had a clear effect on soil desalination [28]. A combination of hydrochemical, hydrogeological and remote sensing analyses was combined to understand the groundwater salinization process of a coastal area. In a further study, between 1990–2020, 223 samples of groundwater were collected and subjected to comprehensive analysis. It was found that salinization was caused by groundwater recharge and active evaporation [29]. Many researchers have worked on the desalination of salt water. In all cases, the method of desalination depends on the purpose of the desalination and the degree of salt concentration required. Some researchers have used industrial techniques such as rubber membranes and osmosis pressures [30, 31], while others have recommended achieving desalination by continuously using fresh water to ensure the renewal of groundwater storage [32].

In summary, the high saline levels in the central area's groundwater are mostly due to the sandy surface soil's high infiltration capacity, which allows for deep percolation. In contrast, the northern and southern areas of the region are distinguished by silty clay surface soils, with little infiltration ability. This helps to keep more water near the surface while maintaining moderate salinity levels.

The goal of this research was to lower the salinity of the aquifer to acceptable TDS levels for agricultural and drinking uses. This was accomplished through a dual mitigation procedure combining the simultaneous pumping of saline water and the injection of freshwater via a network of discharge and recharge wells.

Freshwater, generated solely from the Ishaqi Irrigation Project, was injected into the aquifer via wells located across the area. A portion of the saline water, removed during the discharge process, was reused for irrigation in the northern and southern regions of the Ishaqi region for tolerated plants, where the salinity levels were relatively low. However, in the central region, where salinity was higher, the extracted saline water was redirected and dumped into the southern section of the project.

In general, this study distinguishes itself from earlier studies by providing a mathematical model for desalination in saline aquifers. It is primarily determined by measured levels of aquifer water salinity, using TDS, and storage volume. The precision of the model's inputs, such as the water storage capacity and beginning total quantity of salts, led to precise outputs, such as desalination durations and the appropriate recharging and pumping volumes. Although this study was applied locally, it is considered a mathematical model that can be applied globally, and this technology can be used for desalination in all confined and unconfined saline aquifers, as well as surface reservoirs.

Area of study

The Al-Ishaqi area is located west of the river Tigris, with an area of about 410 km², and its agricultural land is irrigated by surface irrigation [3]. The geographical position lies between longitude (43° 55' 12"– 44° 28' 05") E and latitude (33° 30' 28"– 34° 03' 07") N. The annual rainfall may reach 200mm/year, with the highest level occurring in January. The maximum and minimum temperatures range between 25 and 45°C in summer and 0°C–25°C in winter. The relative humidity ranges between 70 and 80%. The wind speed is 1 m/s in December

and about 3 m/s in March. The sunshine is in the range of 12–14 h/day. Evapotranspiration is 1,700 mm/month [3, 33].

The Ishaqi area is characterized by being flat with an elevation of 45m above sea level (m.a.s.l) and higher than the water level of the Tigris, adjacent to it from the east (Fig. 1). This area remained uncultivated until the Ishaqi Canal was constructed in recent years. The canal takes its water from the Samarra Barrage and carries the water toward the south, meeting all the necessary water demands for the Ishaqi area [34]. From the above, it can be seen that the quality of Ishaqi canal water from a chemical and biological perspective directly affects the quality of groundwater storage of the unconfined aquifer, which is fed by the infiltration of irrigation water through cultivation activities.

The factors that influence infiltration are the soil or the sediment texture, clay mineralogy, depth, pores, channels, residence time, and infiltration rates [35, 36]. The infiltration rate (the cumulative depth of infiltration per time interval) is generally highest when the soil is dry. As the soil becomes wet, the infiltration rate slows to the rate at which water moves through the most restrictive layer, such as a compacted layer or a layer of dense clay. Many researchers have studied the Ishaqi from different aspects, some focusing on the distribution of salinity ratios in the soils, while others have investigated the groundwater suitability for various purposes. Yet others have investigated the environmental assessment of land use in the area [37].

However, the evaluation of the relationship between infiltration and groundwater salinization in this area has not been yet studied. Accordingly, a hydrochemical investigation of the groundwater in the Ishaqi area is essential to address the problem of salinity and suggest suitable solutions to decrease the harmful effects of different saline water uses, especially concerning land irrigation. The geology reveals that the region is covered by quaternary deposits [3]. These deposits consist of sediments filling depressions, formed by the flooding of the Tigris. The sediments are generally made up of fine sand, silt, and clayey silt. The chemical and biological environment of the unconfined aquifer in the Ishaqi area has begun to change over time. In this study, it was decided to identify the causes of the chemical fluctuations of groundwater, which can be attributed to the pollution in the irrigation water originating from the Ishaqi Canal and further agricultural and urban activities.

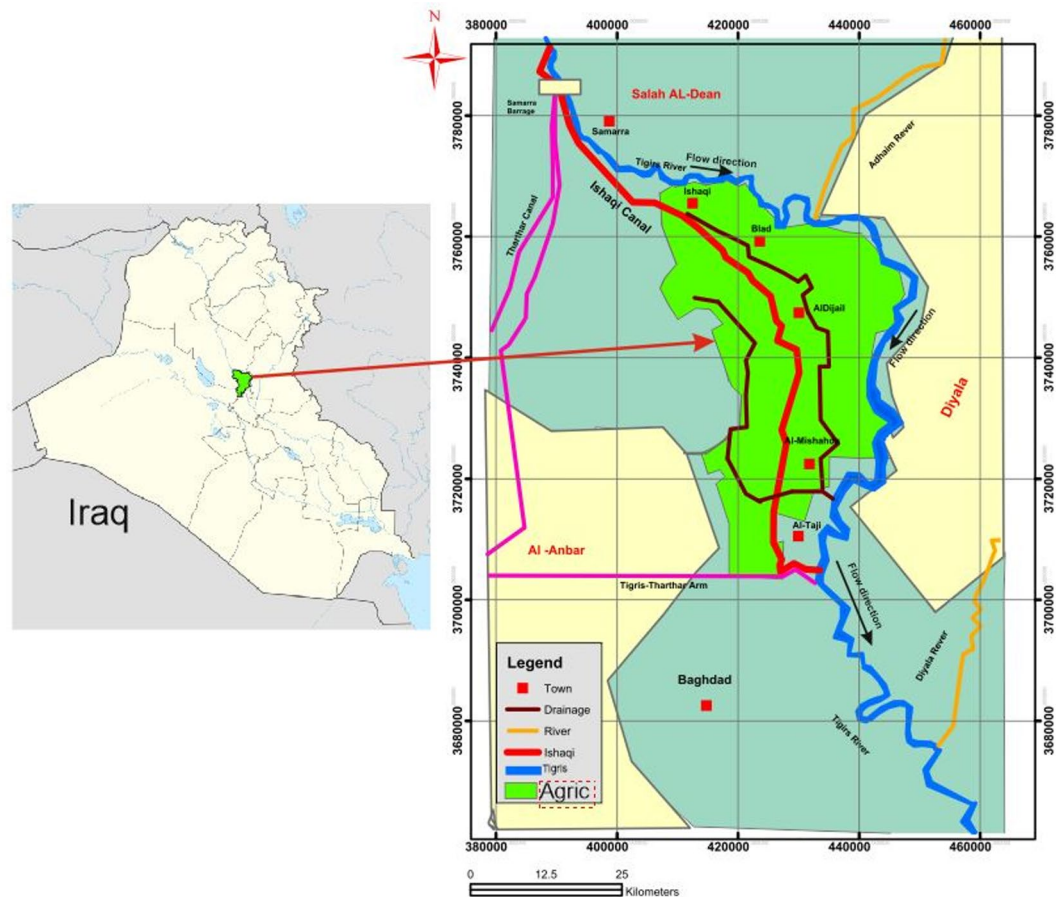


Fig. 1. Location map of Ishaqi area drawn by Surfer™ V.13 <https://support.goldensoftware.com/hc/en-us/articles/226806288-Download-my-software-online> based on the map of Iraq.

Materials and methods

Soil texture analysis

Random soil samples from 10 sites were extracted from the Ishaqi area for a grain size distribution analysis. The test sites were distributed evenly over the entire area, as shown in Fig. 2. The grain size distribution tests included a sieve analysis for coarse aggregates and a hydrometer analysis for fine aggregates (silt and clay). The tests were conducted according to ASTM D 422 specifications [38]. Most of the samples were characterized by fine texture of about 70–80% fine-grained soil, while for sites samples 5 and 6, the soil comprised 95% and 70% coarse-grained sand, respectively. The grain size analysis is shown in (Fig. 3).

It can be seen from Fig. 3, that the soil samples across the considered area were clayey loams. It was anticipated the soil would be silt and silty clay in the northern and southern parts of the region, and sandy soil in the middle [40].

Infiltration power model

Many infiltration models have been created since the Horton model in 1940 [39], three of which are designed to estimate the infiltration potential during the rainstorm or irrigation interval [35, 40]. The *power model* is the most powerful. It has been proven to be a better fit and more applicable for the Mediterranean region in general and Iraq in particular because there are no drawbacks connected to initial low-intensity rainstorms.

The considered model has the following form:

$$f_p(t) = f_c + at^{-k} \quad (1)$$

where $f_p(t)$ is the infiltration rate or infiltration capacity; f_c is a final infiltration rate; t is the infiltration time from the start of the infiltration process; and a and k are coefficients extracted from the infiltration test data. The accumulated infiltration, $AF_p(t)$, is obtained by integrating Eq. 1 to obtain the form:

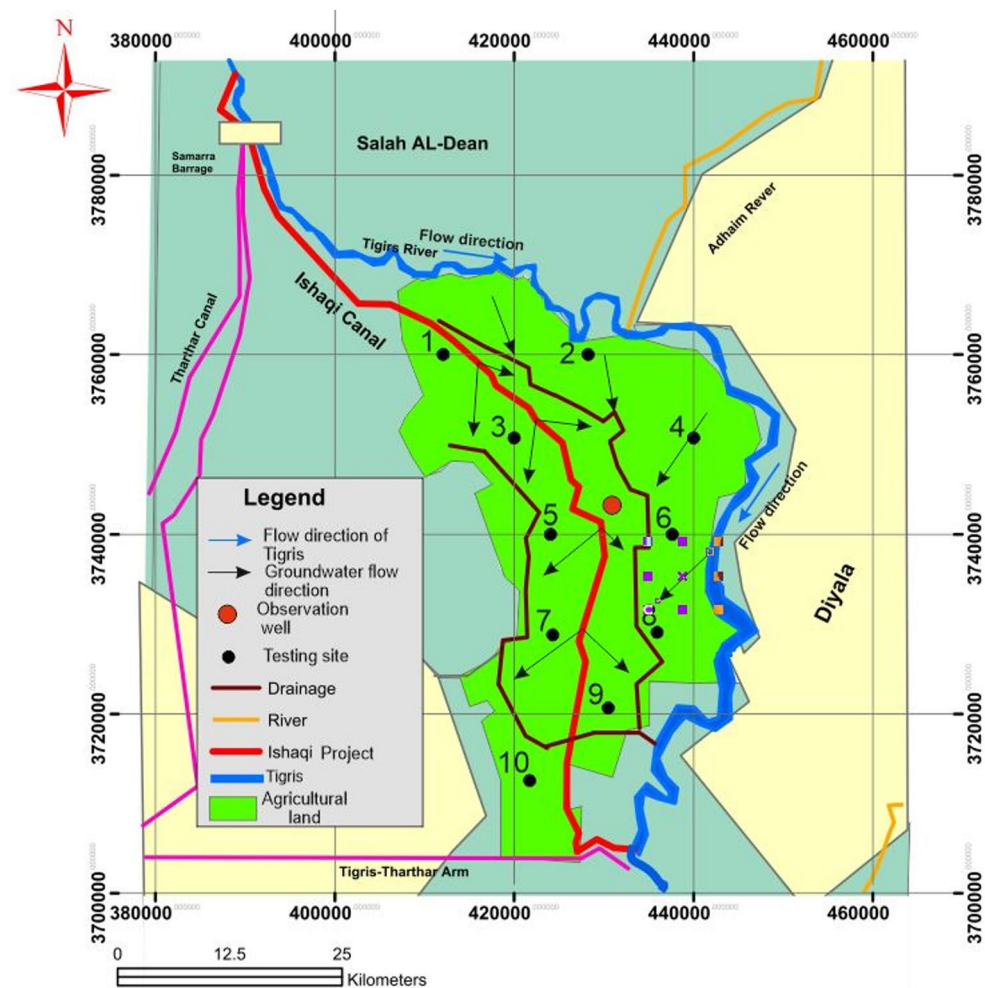


Fig. 2. Testing, sampling observation sites and groundwater flow direction drawn by Surfer™ V.13 <https://support.goldensoftware.com/hc/en-us/articles/226806288-Download-my-software-online> based on the map of Iraq.

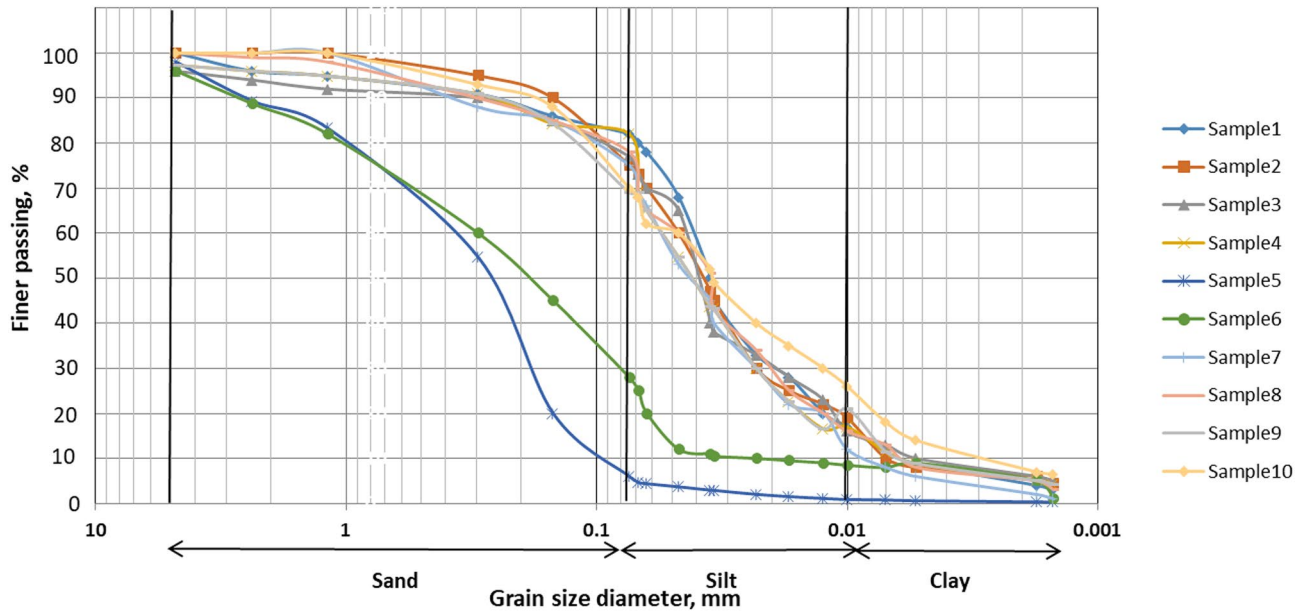


Fig. 3. Grain size analysis of soil samples.

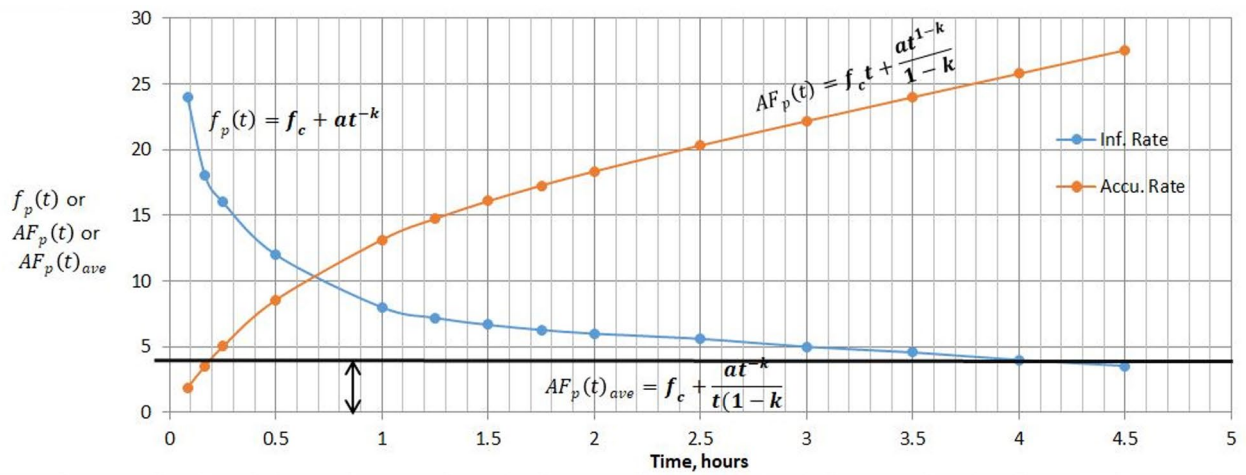


Fig. 4. Infiltration capacity, accumulated infiltration, and average infiltration of the power model.

$$AF_p(t) = f_c t + \frac{at^{1-k}}{1-k} \tag{2}$$

To find an average infiltration rate during a rainstorm, Eq. 2 may be divided by (t), to give;

$$AF_p(t)_{ave} = f_c + \frac{at^{-k}}{(1-k)} \tag{3}$$

To find the coefficients a and k, one may write:

$$k = \log\left(\frac{at}{f_p(t) - f_c}\right) \text{ or } a = (f_p(t) - f_c) t^k \tag{4}$$

The infiltration rate, Eq. 1, the accumulated infiltration or the infiltration capacity, Eq. 2 and the average infiltration rate, Eq. 3, can be represented graphically, as shown in Fig. 4.

Hydrology of the ishaqi canal

The Ishaqi Canal runs from the Samarra Barrage to the Kadhimiya district, North Baghdad, as shown in Fig. 1. It is an open channel, flowing to the right of the Tigris, with a discharge of 80 m³/s. At 30 km distance downstream, it divides into two branches, the eastern and western canals. The borders of the Ishaqi Canal are divided into two districts, with the Baghdad-Mosul Road being the dividing line between them [41]. The total water loss through the infiltration process is about 38.6% of the total water demand for irrigation purposes [3, 42]. The TDS value of Ishaqi water has the same value as 500 mg/L of the Tigris. (Fig. 5).

Mitigation theory and aquifer sustainability

To reduce the salt concentrations of the aquifer in general, it is preferable to inject it with fresh water and pump salty water simultaneously for possible uses such as watering crops that are highly tolerant to salinity. Therefore, if it is assumed that there is an aquifer with a known volume and salt concentration, we can mathematically derive an equation for the aquifer desalinization. The theory of desalinization is based on the following assumptions:

1. The aquifer is enclosed.
2. The groundwater concentration is kept uniform across all the aquifers.
3. The inflowrate concentration < initial concentration of the groundwater.

If the mass of groundwater at any time t is $M(t)$, $M'(t)$ is the concentration difference per time, Q_i is the inflow of salt, C_i is the inflowrate concentration, Q_o is the outflowrate, and V_s is the volume of aquifer storage (Figure 5), as shown in :

$$m'(t) = \text{Salt in flow rate} - \text{Salt out flow rate} \quad (5)$$

$$\text{Salt in flow rate} = Q_i C_i, \text{ and salt out flow rate} = \frac{Q_o}{V_s} M(t)$$

Thus Eq. 5 becomes:

$$= Q_i C_i - \frac{Q_o}{V_s} M(t), \text{ or}$$

$$\frac{dM}{dt} = Q_i C_i - \frac{Q_o}{V_s} M(t)$$

Further rearrangement gives:

$$\frac{dc}{dt} = \frac{dM}{V_s Q_i C_i - Q_o M(t)} = V_s^{-1} \quad (6)$$

The integration of both sides of Eq. 6 offers:

$$\ln([V_s Q_i C_i - Q_o M(t)]) = -\frac{Q_o}{V_s} t + k_1 \text{ or,}$$

$$V_s Q_i C_i - Q_o M(t) = k e^{-\frac{Q_o}{V_s} t} \quad (7)$$

The temporal boundary of the problem may be:

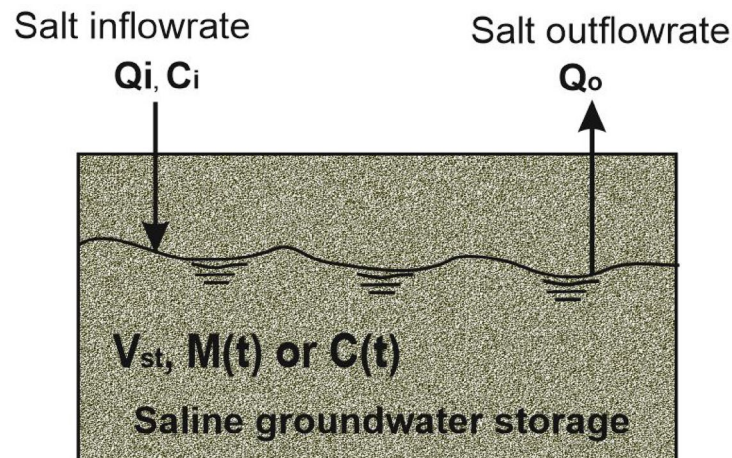


Fig. 5. Inflow and outflow of aquifer salt.

$$[\text{At } t = 0, M(t) = M_{\text{initial}}]$$

Where C_{initial} is the initial salt concentration of the aquifer at the beginning of the mitigation process. Correspondingly, the constant of integration is:

$$k = V_s Q_i C_i - Q_o M_{\text{initial}}$$

By substituting k in Eq. 7, we may obtain the general form of the mitigation equation:

$$M(t) = V_s \frac{Q_i}{Q_o} C_i - \left(V_s \frac{Q_i}{Q_o} C_i - M_{\text{initial}} \right) e^{-\frac{Q_o}{V_s} t} \quad (8)$$

Divide Eq. 8 by the aquifer volume V_s to get:

$$C(t) = \frac{Q_i}{Q_o} C_i - \left(\frac{Q_i}{Q_o} C_i - C_{\text{initial}} \right) e^{-\frac{Q_o}{V_s} t} \quad (9)$$

where $C(t)$ is the groundwater storage concentration at any time t , and C_{initial} is the initial concentration of the groundwater.

By analyzing Eq. 9, one can conclude that:

At $t = 0$, Eq. 9 reduces to $C(0) = C_{\text{initial}}$

$$\text{At } t = \infty, \text{ Eq.9 reduces to } C(\infty) = \frac{Q_i}{Q_o} C_i \quad C(\infty) = C_i \quad (10)$$

which means at the end of the desalination process, the aquifer concentration is equal to the inflowrate concentration.

For simplification of the desalination dynamic of Eq. 9, if it is assumed that $Q_o = Q_i$, Eq. 9 is reduced to:

$$C(t) = C_i - (C_i - C_{\text{initial}}) e^{-\frac{Q_o}{V_s} t} \quad (11)$$

Results and discussion

Chemistry of the Ishaqi region

Studying the effect of the chemistry of the Ishaqi Canal on the salinization of groundwater in the area requires many chemical tests, which are not necessary in this case. The TDS can be considered an indicator of salinization as it represents the total dissolved elements in the canal water that are directly transferred to the groundwater.

Groundwater TDS

TDS, or salinity, represents the total of minerals dissolved in water as cations and anions (ppm) [42]. It is a significant parameter in water quality evaluation. TDS comprises inorganic salt, such as Ca, Mg, Na, K, HCO_3 , Cl, SO_4 , NO_3 , and organic matter that is dissolved in water. The chemical tests in the Ishaqi groundwater revealed that the TDS values ranged between 2,050 and 4,200 Mg/L, as indicated in Table 1. The locations of the sampling sites and TDS values are shown in the contour map (Fig. 6).

From the contour map in Fig. 6, it can be seen that the maximum concentrations of TDS in the groundwater were found in the middle part of the considered area.

Infiltration analysis

The double-ring infiltrometer test was used for measuring infiltration rates in the Ishaqi area according to the specification ASTM D3385-9403 [33, 42]. The same 10 sites in Fig. 2 were used to carry out the double-ring infiltrometer test, which almost covered the entire area. The test was usually repeated three times, using the concept of Eqs. 1, 2, 3 and 4 [36], for each site and the infiltration capacity was obtained and is included in Table 1. The measured infiltrations of the tests are represented in the graphs in Fig. 7.

The estimated average infiltration rates in the selected sites by using Eq. 3 were tabulated (Table 1) and are represented graphically by the contour map (Fig. 8).

From Table 1 and Fig. 8, it can be concluded that the Ishaqi area has the highest infiltration capacity in sites 5 and 6, in the center of the area.

Test site	1	2	3	4	5	6	7	8	9	10
a	7.979393	4.511529	180.2607	16.13605	2.106347	10.99054	6.35507	14.40498	12.28583	4.501313
k	1.2045	1.0995	3.7817	3.0482	1.32514	2.19797	1.2364	1.34722	1.34722	0.87659
$AF_p(t)$, mm/hr	103	87	104	100	183	174	98	107	108	95
TDS, mg/L	2,140	2,100	2,050	2,130	4,200	4,100	2,120	2,160	2,170	2,115

Table 1. Infiltration rate (capacity) and TDS at the Ishaqi Area.

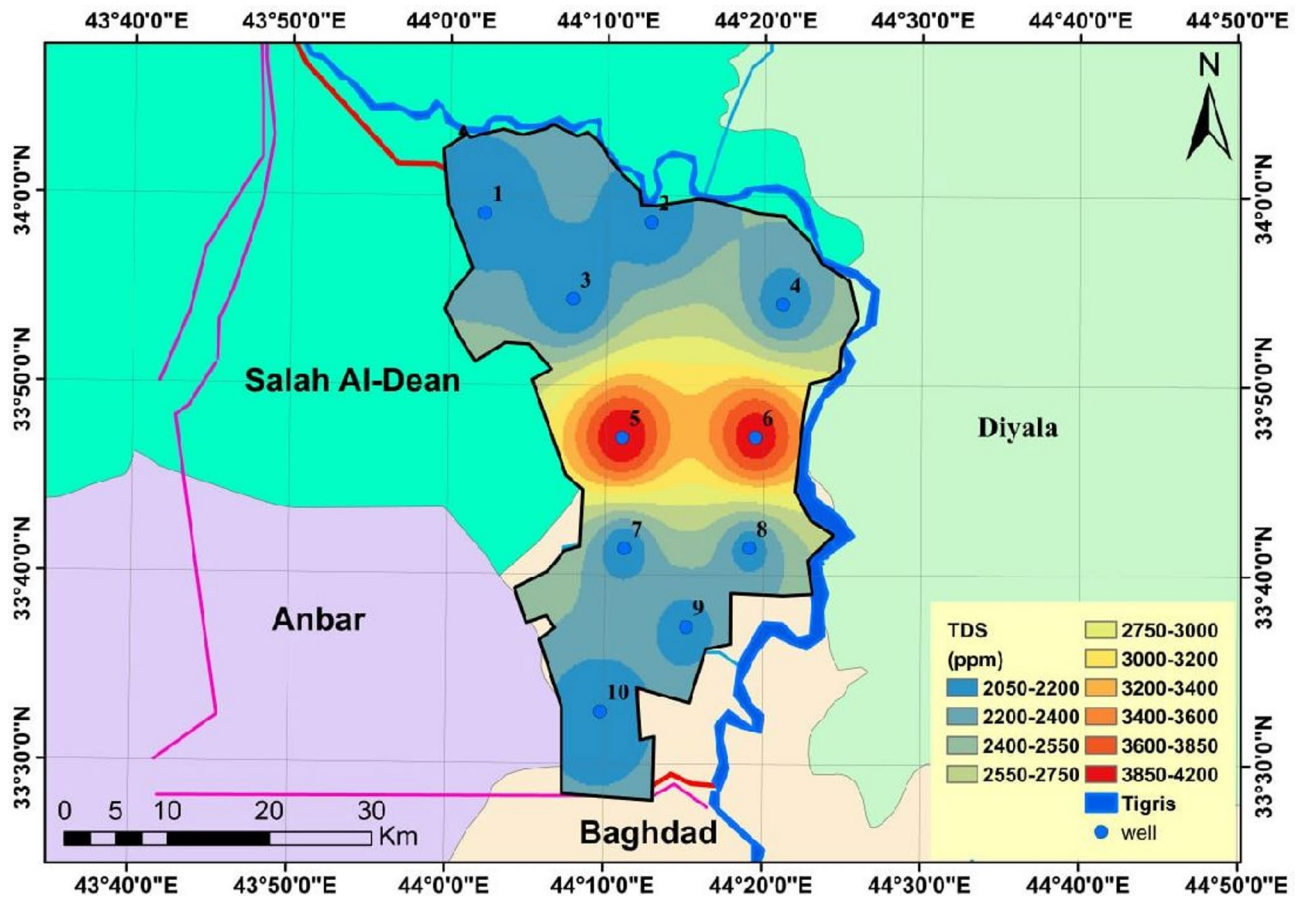


Fig. 6. TDS distribution in Ishaqi groundwater in 2024 drawn by Surfer™ V.13 <https://support.goldensoftware.com/hc/en-us/articles/226806288-Download-my-software-online>.

This high infiltration rate arose due to the coarse texture of soil around the central part of the area, around wells No. 5 and 6. According to the grain size distribution of the surface soil in Fig. 3, an aggregate sample of 5% passing by weight for Well No.5 indicates 95% coarse aggregate (sand), and 30% passing by weight for Well No.6 indicates that 70% coarse aggregate (sand) is retained on sieve No.4. This is an index for high vertical permeability for surface water [36]. The local infiltration rates shown in Fig. 7 confirm these observations. Wells No. 5 and No. 6 exhibit higher infiltration rates than other locations, as illustrated in Fig. 7. Correspondingly, the highest TDS concentration encountered at the central sections of the area are shown in Table 1 for wells No. 5 and 6 (4,200 Mg/L and 4,100 Mg/L, respectively). Similarly, the largest infiltration rates in the middle of the area seen in Table 1 for wells 5 and 6 (183 mm/hr and 174 mm/hr, respectively) can be attributed to the coarseness of the soil's surface layer.

The results reveal that the value of infiltration rate across the considered area ranged between 87–183 mm/hr. These infiltration capacities have a bad impact on the groundwater and its retention of pollution and salinization.

Infiltration-salinization relationship

By matching the contour map of TDS (Fig. 6) and the contour map of infiltration capacity (Fig. 8), it was found that there is a direct relationship between them. The greater the infiltration capacity, the greater the concentration of TDS. The values of Table 1 are represented graphically in Fig. 9. A third-degree mathematical function between the TDS and infiltration capacity was obtained.

Let us assume the average infiltration capacity to be (IC). Then, we have:

$$\text{TDS} = -0.0053(\text{IC})^3 + 2.2546(\text{IC})^2 - 286.16(\text{IC}) + 13445 \quad (12)$$

With correlation coefficient $R^2 = 0.998$.

By applying Eq. 12, one can predict the values of TDS at any location within the Ishaqi region. In general, the main purpose of Fig. 8 is to demonstrate that there is a close and direct relationship between the average infiltration rate and the TDS concentrations.

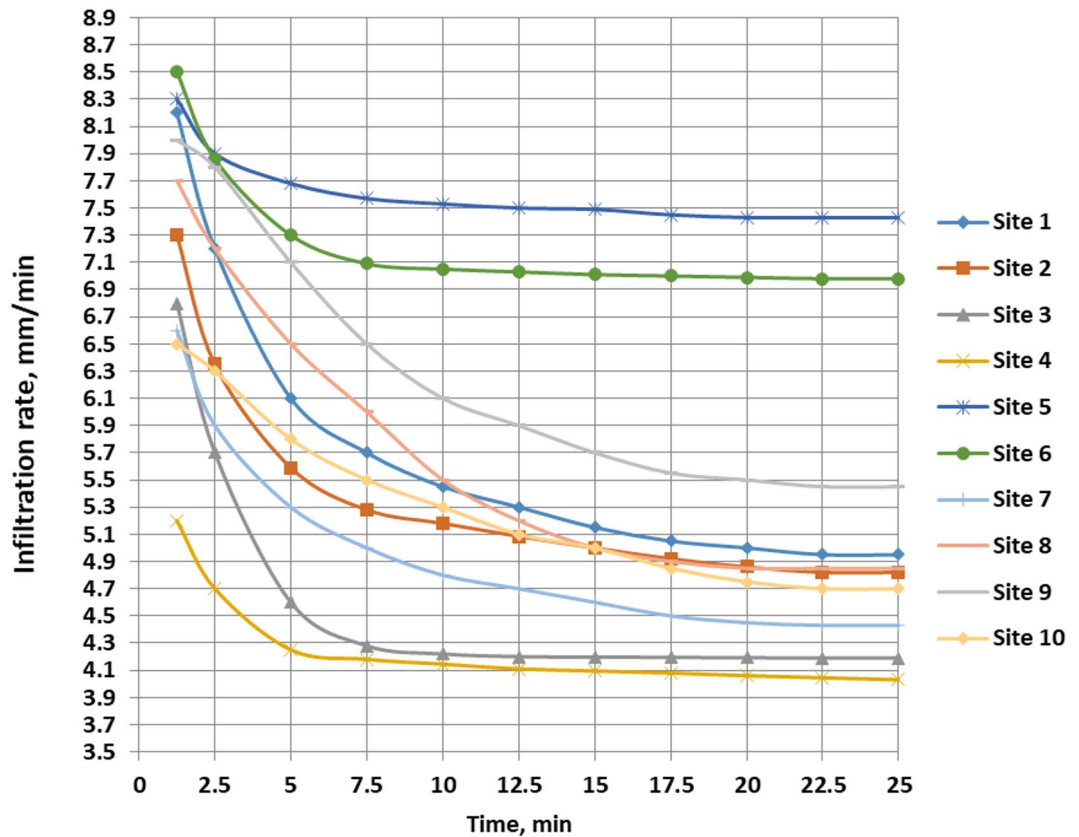


Fig. 7. Measured infiltration.

Sustainable desalination

Plant crop tolerance

Figure 6 shows that TDS reaches 4,200 Mg/L in the middle of the Ishaqi region and declines to 2,000 Mg/L in the northern and southern sections. Table 2 shows that these concentrations are unsuitable for most plant crops. Table 2 reveals that a TDS equal to 500 Mg/L is suitable for all plants [43]. Concentrations higher than 500 Mg/L harmful for sensitive plants..

Table 3 Indicates the common plant crops cultivated in Iraq. It also shows their tolerance levels.

Desalination technique

In the case of the Ishaqi aquifer, the volume of the middle part of the aquifer is 10^8 m^3 [44] and the initial concentration of this part, (see Table 1) is 4,200 mg/L or (4,200 ppm). Equation 9 can be reduced to:

$$C(t) = 500 - (500 - 4,200) e^{-\frac{Q_o}{10^8} t} \begin{bmatrix} C_{\text{initial}} = 4,200 \frac{\text{Mg}}{\text{L}} \\ Q_o = Q_i \\ V_s = 10^8 \text{ m}^3 \\ C_i = 500 \text{ Mg/L} \end{bmatrix} \quad (13)$$

Equation 9 is adopted to mitigate the aquifer concentration from 4,200 Mg/L to 500 Mg/L.

The results of Eq. 9 are represented graphically in Fig. 10.

As indicated in Fig. 10 and Table 4, the dual-action pumping and injection of the Ishaqi aquifer revealed that the initial concentration in the middle part of the aquifer of 4,200 Mg/L could be reduced to the inflowrate concentration of 500 Mg/L by using different pumping rates depending on the plant crop. In the first strategy, five pumping rates were employed: namely, $1 \text{ m}^3/\text{s}$, $2 \text{ m}^3/\text{s}$, ..., $5 \text{ m}^3/\text{s}$. In Table 4, for instance, in pumping rate no.1, if a recharge and discharge rate of $1 \text{ m}^3/\text{s}$ was used to reduce the initial concentration of the aquifer from 4,200 Mg/L to 500 Mg/L, 8,800 days were needed to complete the desalination process. For recharge and discharge using 2, 3, 4, and $5 \text{ m}^3/\text{s}$, the time required to reach a 500 Mg/L concentration was 4,620; 3,140; 2,360; and 1,780 days, respectively (see Table 4). Figure 10 reveals that for the required concentrations of $> 500 \text{ Mg/L}$, less time was needed for the pumping and recharging operation.

In the second strategy, the same input and output data were used except the outflowrate was double the inflowrate rate ($Q_o = 2Q_i, \text{ m}^3/\text{s}$). The results are shown in Table 5 and represented graphically in Fig. 11.

By comparing the periods required for the desalination process in Tables 4 and 5, it can be seen that the time required was much less in the 2nd strategy. For instance, in the first strategy, for pumping rate no.1, the required

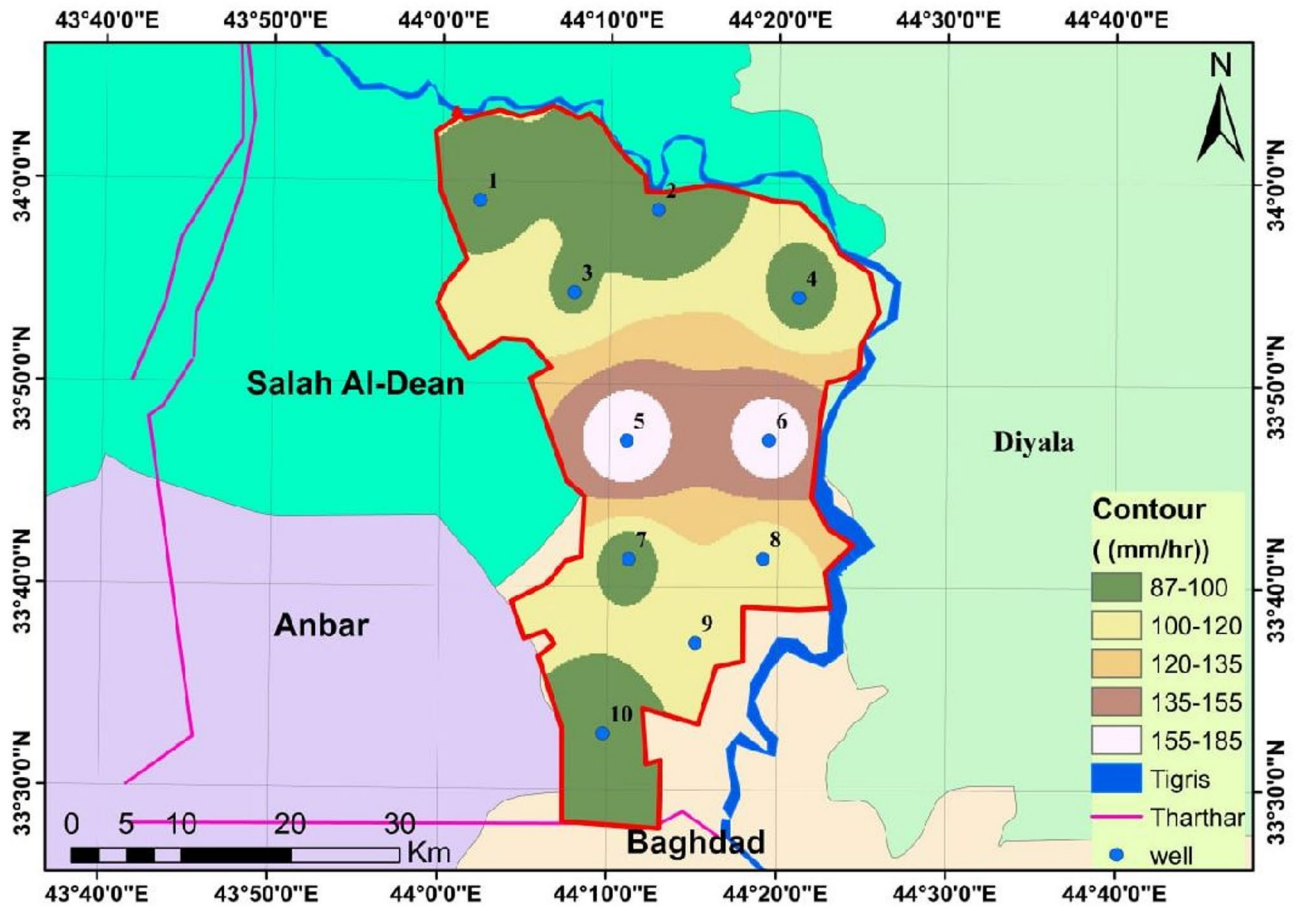


Fig. 8. Contour map of measured infiltration capacity over the Ishaqi area, mm/hr. drawn by Surfer™ V.13 <http://support.goldensoftware.com/hc/en-us/articles/226806288-Download-my-software-online>.

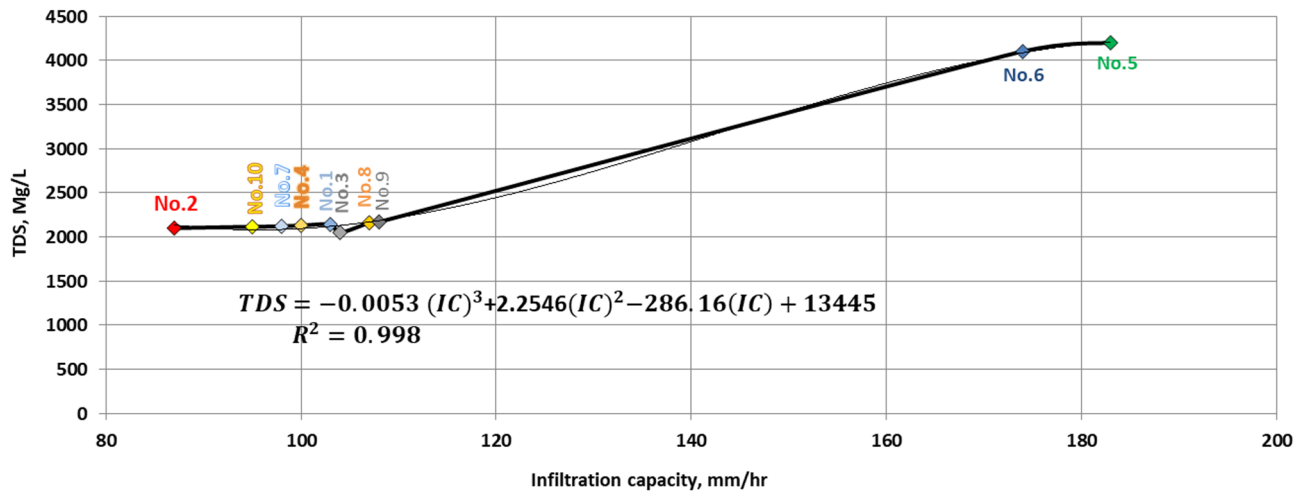


Fig. 9. Infiltration-TDS relationship.

period for the desalination process was 8,800 days, whereas in the second strategy, the required period was 3,190 days.

Analysis of the desalination periods

When comparing Tables 4 and 5, it can be seen that in the 1st strategy—where the recharge and discharge rates were equal ($Q_o=Q_i$) and ranged from 1 to 5 m³/s—the required desalination durations were 24.1; 12.6; 8.6;

TDS	Tolerance	Status
< 500	Excellent	Suitable for all plants
500–1,000	Good	Suitable for moderately salt-sensitive crops
1,000–2,000	Permissible	Suitable for tolerant crops with appropriate management
2,000–3,000	Doubtful	Used only with salt-tolerant crops
> 3,000	Severe	Severe restrictions on use; only very tolerant crops may survive

Table 2. Use of saline water for irrigation purposes, TDS in Mg/L.

Crop	Salinity tolerance	TDS tolerance range, Mg/L
Wheat	Moderate	1,000–2,000
Barely	High	2,000–4,000
Corn	Moderate	1,000–1,500
Cotton	High	2,000–3,000
Rice	Low- Moderate	750–1,500
Date Palm	Very high	Up to 5,000
Tomatoes	Moderate	1,000–1,500
Alfalfa	Moderate	1,000–1,500
Onion	Low	< 1,000
Cucumber	Low	< 1,000
Potatoes	Low-Moderate	500–1,500

Table 3. Common plant crops and their tolerance for TDS concentrations in the Ishaqi Region.

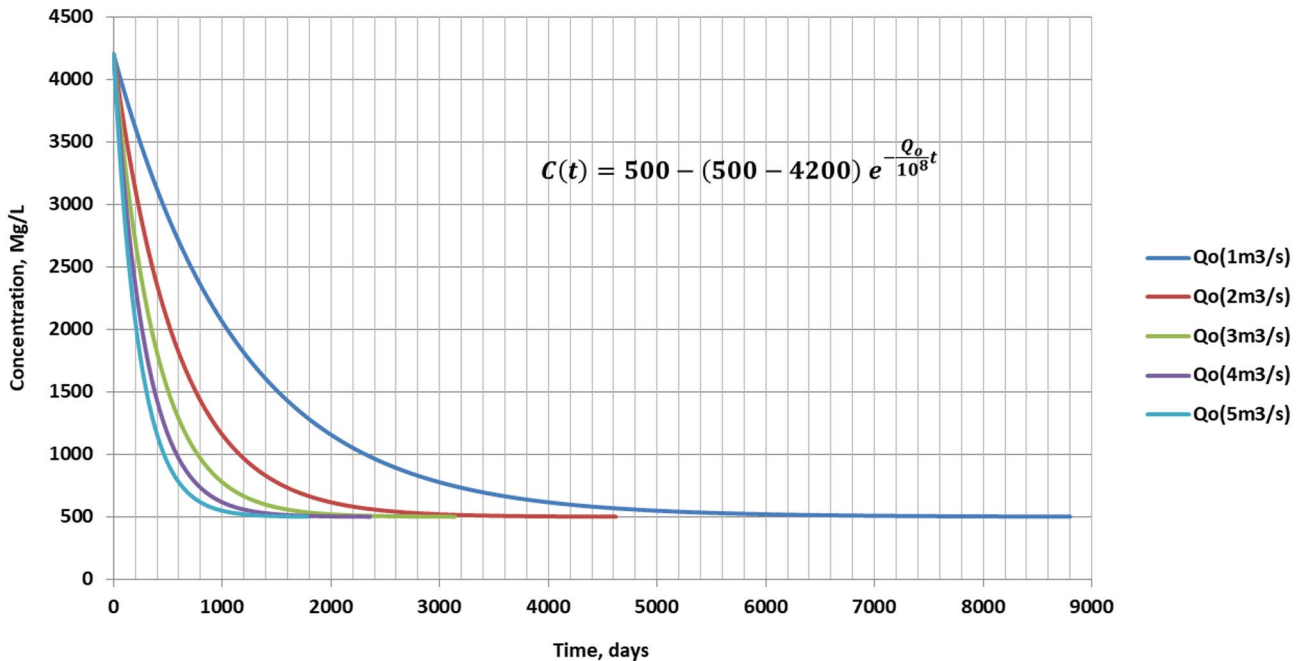


Fig. 10. Aquifer desalination by recharging freshwater and discharging saltwater by using differnt pumping rates, $Q_o = Q_i$, 1st strategy.

6.46; and 4.87 years, respectively. In contrast, when the recharge rates (Q_i) remained fixed at 1 to 5 m³/s and the discharge rates were doubled ($Q_o = 2Q_i$), the required desalination periods significantly decreased to 8.74; 4.38; 2.9; 2.2; and 1.68 years, respectively. This adjustment resulted in an average time reduction of approximately 65.34% between the two strategies, as shown in Table 6.

Pumping rate	$Q_o = Q_i, m^3/s$	Initial concentration, (Mg/L)	Required concentration, (Mg/L)	Time for recharging and pumping rates, days (year)
1	1	4,200	500	8,800 (24.1 years)
2	2			4,620 (12.6 years)
3	3			3,140 (8.6 years)
4	4			2,360 (6.46 years)
5	5			1,780 (4.87 years)

Table 4. The recharging and discharging process of the 1st strategy.

Pumping rate	$Q_o = 2Q_i, m^3/s$	Initial concentration, (Mg/L)	Required concentration, (Mg/L)	Required time for recharging and pumping rate, (days)
1	1	4,200	500	3,190 (8.74 years)
2	2			1,600 (4.38 years)
3	3			1,060 (2.9 years)
4	4			800 (2.2 years)
5	5			680 (1.86 years)

Table 5. The recharging and discharging process of the 2nd strategy.

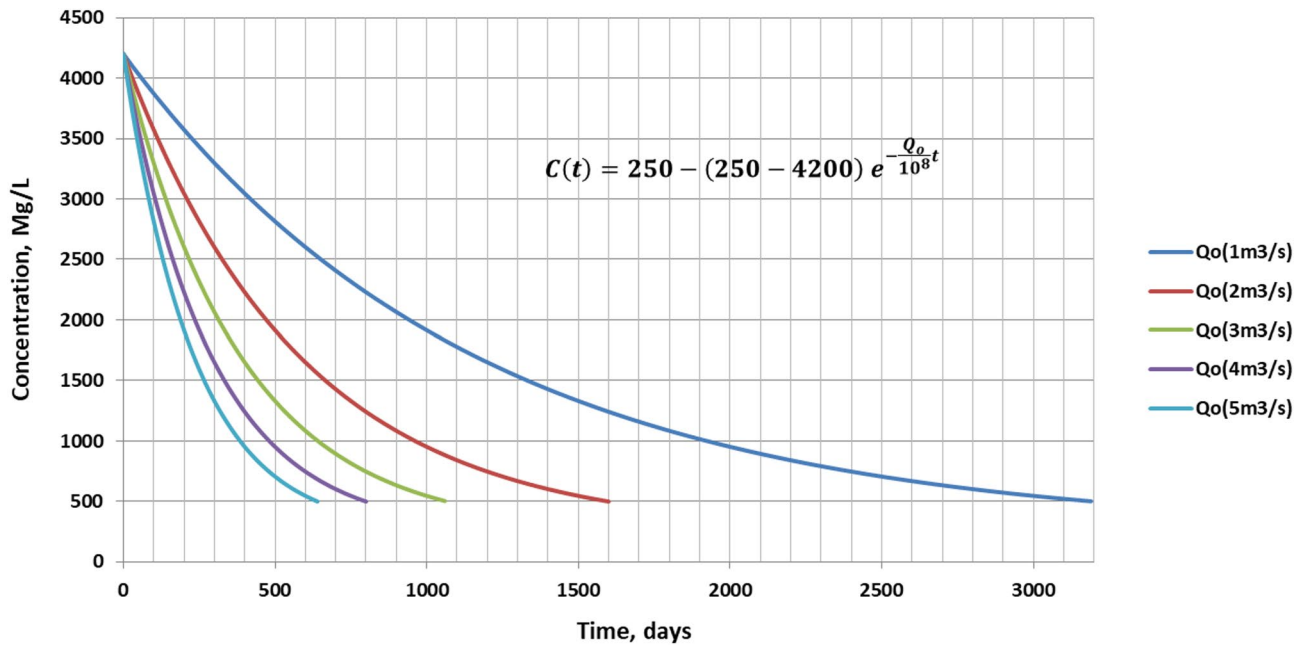


Fig. 11. Aquifer desalination by recharging freshwater and discharging saltwater when using different pumping rates: $Q_o = 2Q_i$, the 2nd strategy.

Recharging rate (Q_i), m^3/s	Desalination period, years		Time reduction%
	1 st strategy, $Q_o = Q_i$	2 nd strategy, $Q_o = 2Q_i$	
1	24.1	8.74	63.73
2	12.6	4.38	65.24
3	8.6	2.9	66.28
4	6.46	2.2	65.94
5	4.87	1.68	65.50
Average			65.34

Table 6. Desalination periods analysis.

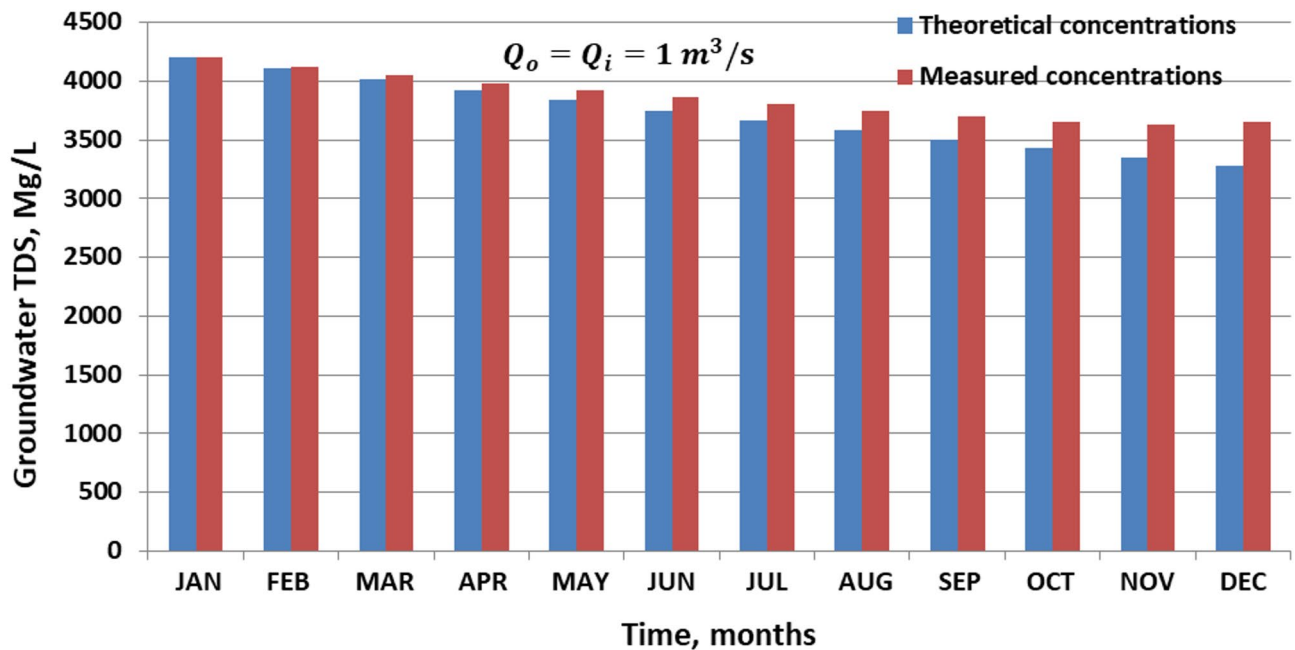


Fig. 12. Comparison between the theoretical and measured concentrations during the desalination process in 2024.

Calibration and verification of the desalination model

The first stage in determining the validity of the desalination theoretical data was to calibrate the model based on the convergence of the theoretical and observed TDS concentrations. This was accomplished by first estimating the aquifer storage volume, $V_S = 369 \times 1,006 \text{ m}^3$, and then running the model. The volume was then adjusted until the theoretical and measured concentrations were in agreement.

The process of abstracting a groundwater sample started in January 2024, when $1 \text{ m}^3/\text{s}$ was injected into 10 wells at the test sites continuously for 24 h per day, as shown in Fig. 2, at a rate of 100 L/second for each injection well in the Ishaqi Irrigation Project with a salt concentration of 500 mg/L, as mentioned previously. At the same time, a monthly sample was taken from the observation well (shown in Fig. 2) to test the TDS over the period from January to December 2024. Agreement was found between the theoretical and actual TDS results measured from the observation well, although they were slightly higher than the theoretical values, with a maximum difference in percentage equal to 4.3%. This may be attributed to the incomplete mixing of the injected water with the groundwater storage (see Fig. 12).

It can also be seen that in November and December, the measured quantities were somewhat higher than the predicted concentrations of 3,625 and 3,650 Mg/L. This was attributed to the rainy season, which increased the influx of fresh water ($\text{TDS} = 0$) into the aquifer storage.

Conclusion

This study has investigated the interplay between infiltration capacity and groundwater salinization dynamics in the Ishaqi aquifer, in central Iraq, and proposed sustainable desalination strategies. It has highlighted the feasibility of sustainable groundwater management in arid regions through engineered recharge-pumping systems. However, assumptions of aquifer enclosure and homogeneous mixing may limit real-world applicability, necessitating further research into heterogeneous aquifer dynamics and long-term monitoring. Implementing these strategies could mitigate the agricultural and socioeconomic impacts of salinization, ensuring water security for Central Iraq. Policymakers and stakeholders are urged to prioritize such interventions to safeguard groundwater resources against escalating salinity threats.

1. Key findings revealed that the middle region, characterized by coarse-grained soils, exhibited the highest infiltration rates (174–183 mm/hr) and TDS concentrations (4,100–4,200 mg/L), driven by rapid deep filtration and salt accumulation.
2. Calibrating the mathematical model can improve the accuracy of estimating aquifer water storage, which is vital for accurate results.
3. A robust mathematical correlation ($R^2 = 0.998$) was established between infiltration capacity and TDS, underscoring the role of soil texture in exacerbating salinization.
4. The proposed dual-action strategy—simultaneous freshwater injection and saline groundwater extraction—proved effective in reducing aquifer salinity from 4,500 mg/L to 500 mg/L for the different intervals of 24.1; 12.6; 8.6; 6.46; and 4.87 years for 1; 2; 3; and 4.5 m^3/s equi recharging-discharging processes.
5. Pumping rates of 1–5 m^3/s achieved desalination within 8,800–1,780 days, with significant time reductions when the outflow rates were double the inflow rates (e.g., 3,190 days at $1 \text{ m}^3/\text{s}$).

6. Field validation demonstrated strong alignment between theoretical predictions and measured TDS values, with minor discrepancies ($\leq 4.3\%$) attributed to incomplete mixing due to complex geological formations and the heterogeneity of the unconfined aquifer.
7. This model is easier to apply in confined aquifers because of the ease of calculating its volume and controlling the pumping and injection operations.
8. The periods required for desalination of the above-mentioned aquifer are for plants with low tolerance of salinity, such as potatoes and onions, which can tolerate concentrations of approximately 500 mg/L. However, highly tolerant crops, such as cotton and barley, require shorter desalination periods: approximately, one year. Palm trees do not require any desalination.

Data availability

Data is provided within the manuscript.

Material availability

All of the material is owned by the authors and/or no permissions are required.

Received: 20 April 2025; Accepted: 24 September 2025

Published online: 30 October 2025

References

1. Perera, H., Jayawardana, C. & Chandrajith, R. Freshwater salinisation: unravelling causes, adaptive mechanisms, ecological impacts, and management strategies. *Environ. Monit. Assess.* **196**(12), 1195. <https://doi.org/10.1007/s10661-024-13388-2> (2024).
2. Polemio, M. & Zuffianò, L. E. Review of utilization management of groundwater at risk of salinization. *J. Water Resour. Plan. Manag.* **146**(9), 03120002. [https://doi.org/10.1061/\(ASCE\)WR.1943-5452.00012](https://doi.org/10.1061/(ASCE)WR.1943-5452.00012) (2020).
3. Sadeq Hameed, A. H. & Al Thamiry, H. A. Evaluation of Al-Ishaqi irrigation project: A case study eastern canal of the project. *Math. Modell. Eng. Problems* **9**(4), 964–970 (2022).
4. Sun, J. et al. Analysis of saline groundwater infiltration into two loam soils. *Land Degrad Dev* **29**(10), 3795–3802. <https://doi.org/10.1002/ldr.3089> (2018).
5. Yu, S. P., Yang, J. S. & Liu, G. M. Effect of clay interlayers on soil water-salt movement in easily-salinized regions. *Adv. Water Sci.* **22**(4), 495–501 (2011).
6. Casanova J, Devau N, & Pettenati M (2016) Managed aquifer recharge: an overview of issues and options. *Integrated groundwater management: Concepts, approaches and challenges*, 413–434.
7. Dillon, P. et al. Sixty years of global progress in managed aquifer recharge. *Hydrogeol. J.* **27**(1), 1–30. <https://doi.org/10.1007/s10040-018-1841-z> (2019).
8. Mehdizadeh, S. S., Badaruddin, S. & Khatibi, S. Abstraction, desalination and recharge method to control seawater intrusion into unconfined coastal aquifers. *Global J. Environ. Sci. Manag.* **5**(1), 107–118. <https://doi.org/10.22034/gjesm.2019.01.09> (2019).
9. Luyun, R. Jr., Momii, K. & Nakagawa, K. Effects of recharge wells and flow barriers on seawater intrusion. *Groundwater* **49**(2), 239–249. <https://doi.org/10.1111/j.1745-6584.2010.00719.x> (2011).
10. Ringleb, J., Sallwey, J. & Stefan, C. Assessment of managed aquifer recharge through modeling—A review. *Water* **8**(12), 579. <https://doi.org/10.3390/w8120579> (2016).
11. Dahlke H E, LaHue G T, Mautner M R, Murphy N P, Patterson N K, Waterhouse H, ... & Foglia I (2018) Managed aquifer recharge as a tool to enhance sustainable groundwater management in California: examples from field and modeling studies. In *Advances in chemical pollution, environmental management and protection* (Vol. 3, pp. 215–275). Elsevier
12. Han, D. et al. A survey of groundwater levels and hydrogeochemistry in irrigated fields in the Karamay Agricultural Development Area, northwest China: Implications for soil and groundwater salinity resulting from surface water transfer for irrigation. *J. Hydrol.* **405**(3–4), 217–234. <https://doi.org/10.1016/j.jhydrol.2011.03.052> (2011).
13. Abdulameer, L. et al. Sustaining Iraq's hidden resource: a review of the strategies for effective groundwater management. *Water Conserv Manag.* **9**(1), 120–131 (2025).
14. Abdulameer, L. et al. Review of artificial intelligence applications in dams and water resources: current trends and future directions. *Manag. Serv.* **11**, 13. <https://doi.org/10.37934/arfmts.128.2.205225> (2025).
15. Abdulameer, L., Al-Dujaili, A. N., Al-Kafaji, M. S., Al Maimuri, N. M. & Shemal, K. Impact of outlets manifold configuration on hydraulic stability and water hammer in pumping stations. *Results Eng.* **26**, 104747. <https://doi.org/10.1016/j.rineng.2025.104747> (2025).
16. De Louw, P. G., Eeman, S., Essink, G. O., Vermue, E. & Post, V. E. Rainwater lens dynamics and mixing between infiltrating rainwater and upward saline groundwater seepage beneath a tile-drained agricultural field. *J. Hydrol.* **501**, 133–145. <https://doi.org/10.1016/j.jhydrol.2013.07.026> (2013).
17. Yakirevich, A. et al. Modeling the impact of solute recycling on groundwater salinization under irrigated lands: A study of the Alto Piura aquifer, Peru. *J. Hydrol.* **482**, 25–39. <https://doi.org/10.1016/j.jhydrol.2012.12.029> (2013).
18. Xie, X., Wang, Y., Li, J., Su, C. & Duan, M. Hydrogeochemical and isotopic investigations on groundwater salinization in the Datong Basin, Northern China I. *JAWRA J. Am. Water Resources Assoc.* **49**(2), 402–414. <https://doi.org/10.1111/jawr.12028> (2013).
19. Liu, Y., Jin, M. & Wang, J. Insights into groundwater salinization from hydrogeochemical and isotopic evidence in an arid inland basin. *Hydrol. Process.* **32**(20), 3108–3127. <https://doi.org/10.1002/hyp.13243> (2018).
20. Cherschian, SC (2019). Effect of water application methods on salinity leaching efficiency in soils of different textures. University of California, Riverside ProQuest Dissertations & Theses, 13896901.
21. Shi, M. et al. Desalination of saline groundwater by a weakly permeable clay stratum: A case study in the North China Plain. *Environ. Earth Sci.* **78**, 1–13. <https://doi.org/10.1007/s12665-019-8558-8> (2019).
22. Jabbar, D. N. et al. Hydraulic conductivity determination by infiltration models in unsaturated soils overlying shallow groundwater regimes. *Arab. J. Geosci.* **14**(19), 1981. <https://doi.org/10.1007/s12517-021-08273-y> (2021).
23. Miao, Q. et al. Effects of sand addition to heavy saline-alkali soil on the infiltration and salt leaching in hetao irrigation district, China. *Biol. Life Sci. Forum.* **3**(1), 33. <https://doi.org/10.3390/IECAG2021-10156> (2021).
24. Ali, A. R., Jabbar, D. N., Abood, K. F. & Al Maimuri, N. M. Water Phase inclination theory for hydraulic conductivity determination of vadose zones in shallow water table systems. *Iraqi Geol. J.* <https://doi.org/10.46717/igj.54.2B.8Ms-2021-08-28> (2021).
25. He, Y., Wang, Y., Liu, Y., Peng, B. & Wang, G. Focus on the nonlinear infiltration process in deep vadose zone. *Earth-Sci. Rev.* **252**, 104719. <https://doi.org/10.1016/j.earscrv.2024.104719> (2024).
26. Farias, I., Oude Essink, G. H., de Louw, P. G. & Bierkens, M. F. Effects of grid resolution on regional modelled groundwater salinity and salt fluxes to surface water. *J. Hydrol.* **643**, 131915. <https://doi.org/10.1016/j.jhydrol.2024.131915> (2024).

27. Celleri, C., Pratolongo, P. & Arena, M. Spatial and temporal patterns of soil salinization in shallow groundwater environments of the Bahía Blanca estuary: Influence of topography and land use. *Land Degrad. Dev.* **33**(3), 470–483. <https://doi.org/10.1002/ldr.4162> (2022).
28. Guo, K. & Liu, X. The successive infiltration of various saline waters accelerates the infiltration processes and enhances the salt leaching in a coastal saline soil. *Land Degrad. Dev.* **34**(16), 5083–5595. <https://doi.org/10.1002/ldr.4831> (2023).
29. Ouarani, M. et al. A comprehensive overview of groundwater salinization and recharge processes in a semi-arid coastal aquifer (Essaouira, Morocco). *J. Hydrol.: Reg. Stud.* **49**, 101501. <https://doi.org/10.1016/j.ejrh.2023.101501> (2023).
30. Ahdab YD, Lienhard JH (2021) Desalination of brackish groundwater to improve water quality and water supply. In *Global Groundwater* (pp. 559–575). Elsevier. <https://doi.org/10.1016/j.gsd.2020.100506>
31. Prajapati, M. et al. Geothermal-solar integrated groundwater desalination system: Current status and future perspective. *Groundw. Sustain. Dev.* **1**(12), 100506. <https://doi.org/10.1016/j.gsd.2020.100506> (2021).
32. Gude, V. G. Desalination of deep groundwater aquifers for freshwater supplies—challenges and strategies. *Groundw. Sustain. Dev.* **1**(6), 87–92. <https://doi.org/10.1016/j.gsd.2017.11.002> (2018).
33. Al-Majmai, G. S. S., Abdul-Jabar, R. A., & Ali, S. F. (2023, May). Physical and chemical characterization of water in irrigation Al-Ishaqi project. In *AIP Conference Proceedings* (Vol. 2593, No. 1). AIP Publishing. <https://doi.org/10.1063/5.0139832>
34. Abdullah, M., Al-Ansari, N. & Laue, J. Water resources projects in Iraq: Irrigation projects on Tigris. *J. Earth Sci. Geotech. Eng.* **9**(4), 201–230 (2019).
35. Al Maimuri, N. M. Applicability of Horton model and recharge evaluation in irrigated arid Mesopotamian soils of Hashimiya. *Iraq. Arabian J. Geosci.* **11**(20), 610. <https://doi.org/10.1007/s12517-018-3986-4> (2018).
36. Ali, A. R., Hussein, A. A., Abood, K. F. & Al Maimuri, N. M. Sensitivity of infiltration models in rural soils overlying unsteady shallow groundwater. *The Iraqi Geol. J.* **56**, 43–57. <https://doi.org/10.46717/igj.56.1D.4ms-2023-4-13> (2023).
37. Gonella, M., Pretner, A., Lecollinet, J. & Cattarossi, A. Iraq water resources evaluation: an overview of the existing conditions. *Crit. Transit. Water Environ. Resources Manag.* **5**, 1–10. [https://doi.org/10.1061/40737\(2004\)2](https://doi.org/10.1061/40737(2004)2) (2004).
38. ASTM International. (2009). Standard test method for infiltration rate of soils in field using double-ring infiltrometer. ASTM International.
39. Horton, R. E. An approach toward a physical interpretation of infiltration capacity. *Proc. Soil Sci. Soc. Am.* **5**, 399–417. <https://doi.org/10.1002/ldr.4831> (1940).
40. Linsely RK, and Franzini JB (1972). *Water- Resources Engineering*, McGRAW-Hill. NewYork San Francisco. ,sec "Materials and methods". "Introduction", PP, 44.
41. Sulaiman, S. O., Kamel, A. H., Sayl, K. N. & Alfadhel, M. Y. Water resources management and sustainability over the Western desert of Iraq. *Environ. Earth Sci.* **78**(16), 495. <https://doi.org/10.1007/s12665-019-8510-y> (2019).
42. Sadeq Hameed, A. H. & Al Thamiry, H. A. Evaluation the Western Canal of Al-Ishaqi Irrigation Project. *J. Eng. (17264073)*. **29**(5), 13. <https://doi.org/10.31026/j.eng.2023.05.02> (2023).
43. Ayers, R. S., & Westcot, D. W. (1985). *Water quality for agriculture* (Vol. 29, p. 174). Rome: Food and agriculture organization of the United Nations.
44. Jassim, S. Z. & Goff, J. C. *Geology of Iraq* (Prague and Moravian Museum, Brno, Czech Republic, 2006).

Author contributions

N. M. L. designed the study and wrote the main manuscript text. Z.N. Material preparation and data collection. L. A. and A. J. Data analysis. H.J. and A.N. checked the results and validation. All authors reviewed the manuscript. I confirm the corresponding author has read the journal policies and submit this manuscript in accordance with those policies.

Funding

This research received no specific grant from any funding agency in the public, commercial, or not-for-profit sectors.

Declarations

Competing interests

We declare that the authors have no competing interests as defined by Nature Research, or other interests that might be perceived to influence the results and/or discussion reported in this paper.

Dual publication

The results/data/figures in this manuscript have not been published elsewhere, nor are they under consideration (from you or one of your Contributing Authors) by another publisher.

Additional information

Correspondence and requests for materials should be addressed to L.A. or A.N.A.-D.

Reprints and permissions information is available at www.nature.com/reprints.

Publisher's note Springer Nature remains neutral with regard to jurisdictional claims in published maps and institutional affiliations.

Open Access This article is licensed under a Creative Commons Attribution-NonCommercial-NoDerivatives 4.0 International License, which permits any non-commercial use, sharing, distribution and reproduction in any medium or format, as long as you give appropriate credit to the original author(s) and the source, provide a link to the Creative Commons licence, and indicate if you modified the licensed material. You do not have permission under this licence to share adapted material derived from this article or parts of it. The images or other third party material in this article are included in the article's Creative Commons licence, unless indicated otherwise in a credit line to the material. If material is not included in the article's Creative Commons licence and your intended use is not permitted by statutory regulation or exceeds the permitted use, you will need to obtain permission directly from the copyright holder. To view a copy of this licence, visit <http://creativecommons.org/licenses/by-nc-nd/4.0/>.

© The Author(s) 2025